XLI CILAMCE
XLI Ibero-Latin American Congress on Computational Methods in Engineering
16-19 November, 2020 FOZ DO IGUAÇU PARANÁ - BRAZIL

Design and fatigue assessment of gravity base foundations for offshore wind turbines

Gabriel Nogueira[1], Fellipe A. Gomes[1], Eduardo Dorscheidt[1], Gilberto B. Ellwanger[1]

[1]*Dept. of Civil Engineering, Federal University of Rio de Janeiro*
Av. Athos da Silveira Ramos, 149, 21941-909, Ilha do Fundão, Rio de Janeiro, Brazil
gabrielnogueira@coc.ufrj.br, fellipe.gomes@coc.ufrj.br, eduardo.dorscheidt@coc.ufrj.br, gbe@coc.ufrj.br

Abstract. In this work, a gravity base foundation (GBF) was designed to support the DTU's 10 MW wind turbine. Recently, the industry is considering GBFs as a potential solution to the difficulties of driving monopile foundations in certain types of soil. Also, checking their feasibility in greater water depths is a pivotal question since these concrete structures might be cheaper than the steel monopile alternative. Thus, in a 40 meters water depth, the proposed model is checked for its geotechnical capacity and the resistance of critical points under extreme loads. The foundation is designed with a natural frequency that avoids excessive fatigue damage due to the action of Brazilian environmental loads and rotor operation frequencies. This paper discusses the most influential factors in these analyses. Palmgren-Miner rule assessed the fatigue damage in association with the widely employed S-N curves for concrete. SIMA-RIFLEX's dynamic analysis module generated the stress time series. Rainflow method, combined with the Markov matrix, is utilized for counting stress cycles.

Keywords: Wind turbine, Gravity base foundation, Ultimate limit state, Fatigue limit state.

1 Introduction

In Brazil, one of the fastest-growing energy sources at the moment is wind energy. The Brazilian Energy Review of 2020 [1] highlighted this fact by stating an increase of 15.5% of the internal electricity supply from 2018 (48.5 TWh) to 2019 (56 TWh) from this source. All this wind power supply (15 GW of installed capacity [1]) comes from onshore wind farms since Brazil is yet to develop offshore wind projects. According to Amarante *et al*. [2], the onshore wind source potential could reach 143.5 GW at a 50 m height. However, Silva *et al*. [3] state that the Brazilian offshore potential revolves around 1.3 TW in shallow waters (up to 50 m water depth), which is almost ten times over the onshore one.

In the European offshore wind energy industry, the most employed fixed foundation is the monopile, responding for 70% of the newly-installed foundations of 2019 [4]. Despite its success in the market, this support structure has drawbacks in specific situations. Monopile refusal in hard soils is one example. Driving a large diameter foundation in calcareous soils, such as those found along the Brazilian coast, could be challenging, requiring the usage of more sophisticated methods [5]. It is also unsure how much skin friction, and consequently bearing capacity, is available through the grouted driven piles alternative [6] since the external diameters of these structures have been increasing with time.

A potential solution for this issue is the adoption of gravity base foundations, which are typically employed in water depths up to 15 m. In addition to not being necessary to penetrate the soil, concrete is the most commonly used material for GBFs, which can lower the foundation prices when compared to the steel monopile alternative. As stated by Koekkoek [7], materials for concrete GBFs are seven to eight times lower than the steel monopiles per tonne. On the other hand, GBFs can be four to five times heavier than monopiles. Even considering this weight difference, GBFs are a promising possibility in greater water depths.

Therefore, this paper's objective is to design a GBF to support a high power-rating wind turbine developed by the Technical University of Denmark (DTU) [8] under the action of Brazilian environmental loads in a 40 m water depth. The next section presents the considerations made for modeling the turbine and the environmental loads. Then, an Ultimate Limit State (ULS) and geotechnical capacity checks will be made following Koekkoek's work [7] and DNVGL standard [9]. Finally, another verification is carried out for the Fatigue Limit State (FLS). The characteristic compressive strength of concrete will be varied at the end of this last topic to perform a sensitivity study on the foundation's lifespan. The conclusion discusses the most influential factors in all these analyses.

2 Wind turbine model

2.1 Turbine and foundation properties

Figure 1 shows the wind turbine modeled in SIMA-RIFLEX [10] and a detailed scheme of the GBF's geometry. The DTU's 10 MW wind turbine has a 178.3 m rotor diameter and a 119 m hub height. DTU's exact rotor-nacelle assembly was modeled in RIFLEX, and its complete description is available at Bak *et al*. [8]. This work preserved the outer diameter and thickness from the tower top to its base. The tower's length, however, was shortened by five meters when compared to DTU's report [8]. The steel's mechanical properties composing the tower are also found in the report [8]. The GBF is made of reinforced concrete with a mass density of 2500 kg/m³. The characteristic compressive strength of concrete is equal to 55 MPa, and the steel bars are CA-50 [11]. Shear and Young's moduli are equal to 19 GPa and 45.7 GPa, respectively.

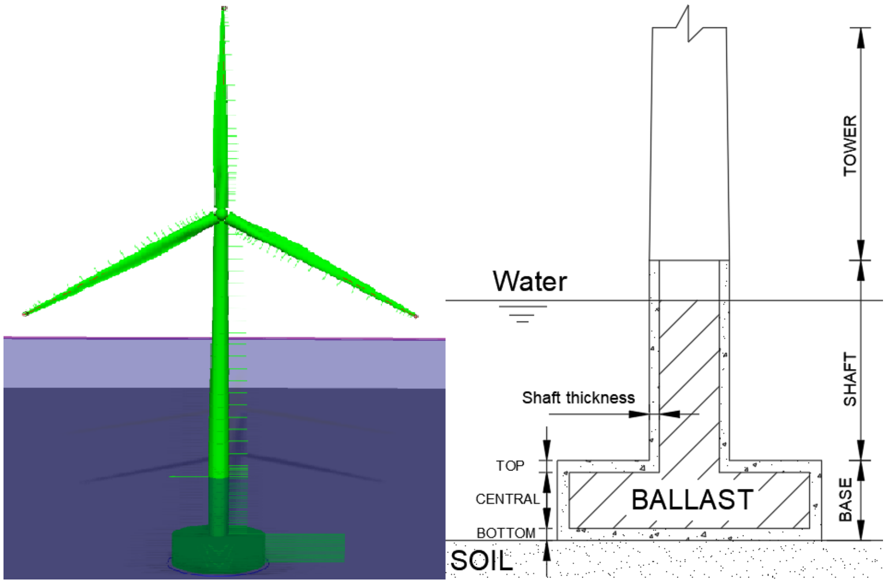

Figure 1. Left: Model in SIMA-RIFLEX. Right: Scheme of the GBF's geometry.

Koekkoek's work [7] helped to create the GBF's dimensions. Even though his model is in a 25 m water depth, the base and shaft diameter-thickness ratios offered a starting point for the development of the structure. Table 1 presents these dimensions.

Table 1. Tower and GBF dimensions.

Section	Length [m]	Ext. diameter [m]	Thickness [m]
Tower	110.63	5.5 (top) – 8.3 (base)	0.02 (top) – 0.038 (base)
Dry shaft	5.00	8.30	1.00
Submerged shaft	26.5	8.30	1.00
Base (top)	1.50	35.0	-
Base (central)	10.5	35.0	1.00
Base (bottom)	1.50	35.0	-

2.2 Environmental loads representation

The Design Load Cases (DLC) selected for this study are DLC 1.2 for FLS and DLC 1.6 for ULS checks, as defined in DNVGL-ST-0437 [12]. These two DLCs represent a significant portion of environments that a wind turbine will experience over its lifespan without simulating all of the possibilities presented in the standard [12]. The Brazilian Northeast environment provides the necessary sea states and wind conditions for the composition of twelve fatigue load cases according to DLC 1.2, as previously done in Nogueira [13] (Table 2). In other words, the significant wave height H_s, wave's peak period T_p, and mean wind speed at a 10 m height U_{10} were retrieved from that work [13]. The ULS check (DLC 1.6) adopts H_s = 3.82 m and T_p = 8.83 s. The chosen wind speed for this case is 11 m/s at hub height, as it causes the greatest thrust force, and the sea current is a uniform profile equal to 0.8 m/s. This paper also utilizes the Jonswap wave spectrum as in Nogueira [13] (peakedness parameter γ = 3.3). SIMA-RIFLEX is capable of creating an irregular sea through the superposition of regular waves, and TurbSim software [14] can export a realistic wind to RIFLEX.

Table 2. FLS loading cases and their occurrences [13].

Case	Direction	U_{10} (m/s)	H_S (m)	T_P (s)	Occurrence (%)
1	N	5	0.7	3.6	0.21
2	NE	7	1.2	4.6	2.15
3	E	9	1.6	5.4	21.86
4	E	12	2.2	6.3	13.82
5	E	13	2.4	6.6	9.08
6	SE	8	0.7	3.4	22.52
7	SE	10	0.9	3.7	16.87
8	SE	11	1.0	3.9	12.17
9	S	6	0.4	2.7	1.13
10	SW	5	0.4	2.6	0.08
11	W	5	0.7	3.6	0.05
12	NW	5	0.7	3.6	0.06

A power-law profile with a 0.056 exponent represents the mean wind speed portion. At the same time, a 5.9% turbulence intensity is assumed in all DLCs (Normal Turbulence Model) to represent the wind's dynamic parcel with the Kaimal's spectrum. A 39x39 grid (237 m x 237 m) is defined in TurbSim to envelop the rotor and the tower completely. The first 400 s of the complete analysis (4000 s) are discarded as they show a transient response. Morison's formulation calculated the hydrodynamic forces in the ULS check (drag and inertia coefficients equal 1 and 2, respectively) while in the FLS check, MacCamy-Fuchs is utilized. The aerodynamic drag coefficient of the tower is 0.6.

2.3 Soil-foundation interaction and resonance check

DNVGL-ST-0126 [9] defines in Appendix G the equations necessary to compose springs that will represent the soil-foundation stiffness. This paper assumed a uniform layer of sand (Poisson's ratio and Young's modulus equal to 0.3 and 30 MPa, respectively) and a considerable distance until bedrock is found, which simplifies the equations presented in the standard [9]. This sand has an angle of internal friction of 28º, 5 kN/m² of cohesion, and 10 kN/m³ of submerged specific weight.

A designer of offshore wind turbines (OWT) must be aware of the environmental loads and rotor operation frequencies. The soft-stiff range is the designer's desired region to steer clear of these frequencies and also avoid an excessively expensive project. The DTU's 10 MW wind turbine soft-stiff region is 0.168 – 0.285 Hz. This area is defined by the rotor operational frequencies (6 to 9.6 rpm) and a five percent margin [9]. This zone and the soil properties strongly influenced the GBF's base diameter (35 m). With these dimensions and properties, the first natural frequencies of this OWT are 0.212 Hz. Therefore, the design is in the soft-stiff region, and resonant effects have been avoided successfully.

3 Ultimate Limit State and Geotechnical Capacity

Table 3 shows the loadings obtained by SIMA-RIFLEX for DLC 1.6. The critical points highlighted in this table are the lowest points of the shaft and the base (Fig. 1). The ULS and geotechnical capacity verification procedures followed Koekkoek [7] and the DNVGL standard [9]. Therefore, the topics evaluated were: calculation of the ultimate bending capacity of the shaft, calculation of maximum crack width, verification of the turning over resistance, calculation of horizontal sliding resistance, and, lastly, bearing capacity of the soil. The safety factors adopted for concrete, steel, and environmental loads were 1.5, 1.15, and 1.35, respectively [7][15].

Table 3. Loadings at critical points of the foundation.

Section	Shaft	Base
Loadings		
Vertical (kN)	2.42E+04	7.81E+04
Horizontal (kN)	6.16E+03	1.93E+04
Torsion (kN.m)	5.79E+03	5.79E+03
Bending Moment (kN.m)	3.24E+05	4.85E+05

3.1 Calculation of the ultimate bending capacity of the shaft and maximum crack width

According to Koekkoek [7], to certify the GBF's ultimate bending capacity, it is necessary to analyze its critical section. This section is located on the shaft-base interface. Although the bending moment at the base is greater, the interface's value is close to it. Also, the cross-section at this point is considerably smaller than at the base. Therefore, we have the GBF's critical point at the interface. A conservative hypothesis adopted for the design of this section is to disregard the structure's weight and analyze it only under the action of the bending moment [7].

The GBF's critical section was modeled in the "Pcalc!" software [16]. It was assumed a 5 cm reinforcement cover (Environmental Aggressiveness Class IV for pillars [11]) and a 2.25 coefficient that governs the bond between concrete and steel bars. During the iterations to conceive the diameter and spacing of the reinforcement bars, it was taken into account that the choice of these properties affects the crack width that will form around the most requested bar.

The designed reinforcement includes 2.5 cm diameter bars, spaced 10 cm apart. Four external layers and three internal ones were necessary to meet the ultimate bending capacity and maximum crack width (0.2 mm [11]). The total reinforcement in this cross-section is 0.634 m² (1291 bars) and is in the appropriate range between the minimum and maximum reinforcement (0.092 – 1.835 m² [11]). This design resulted in a safety factor equal to 2.06, and maximum crack width of 0.165 mm (Fig. 2).

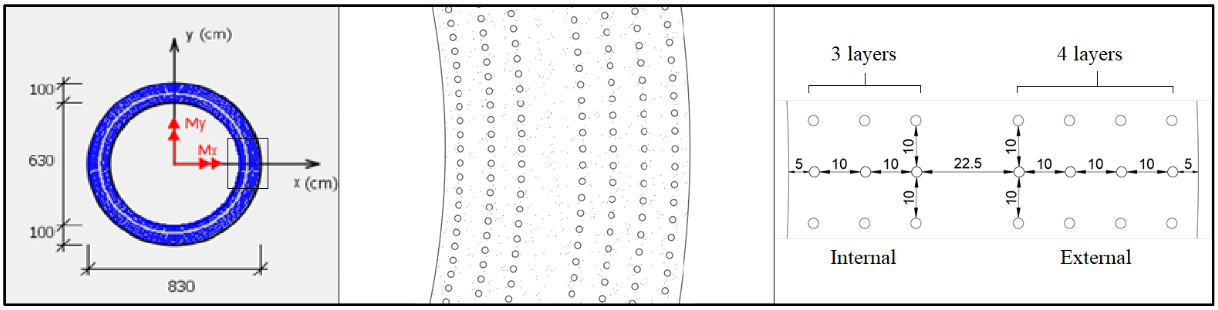

Figure 2. Left: Critical Section in "Pcalc!" [16]. Center: Zoomed cross-sectional view. Right: Detailed scheme of the reinforcement.

3.2 Verification of the turning over resistance

For this verification, the base's bending moment is utilized. Two forces compose the resistance to this loading. One of them is the total weight of this offshore wind turbine discounted from the buoyancy. The soil's reaction to being compressed is the other. The ballast initially adopted in the SIMA-RIFLEX model was seawater (1025 kg/m³ mass density). A spreadsheet, according to Koekkoek's work [7], performed the calculations that determined whether the structure's weight was sufficient or not to contain the turning over bending moment.

After calculating the required weight, the ULS value is obtained by dividing it by 0.9 [7]. The vertical loading obtained was 7.81E+04 kN, which is not enough to meet the ULS value (8.44E+04 kN). Approximately 200 m³ of iron ore (3200 kg/m³ mass density) replaced part of the seawater ballast, making the structure reach the necessary ULS weight.

3.3 Calculation of bearing capacity and horizontal sliding resistance

The horizontal force H (1.93E + 04) and vertical force V (8.44E + 04 kN) of the soil-foundation interface are used in this verification. They are transformed into design forces, namely H_d and V_d. To obtain them, they are multiplied by 1.35, as previously defined. The load center is the point where the resultant of H_d and V_d intercepts the soil-foundation interface, which implies an eccentricity of the vertical force V_d about the centerline of the foundation [9]. For the bearing capacity analysis, it is necessary to calculate this eccentricity and an effective area of the foundation. This area is constructed in a way that its geometric center coincides with the load center (Fig. 3). Additionally, it must follow as closely as possible the contour of the base [9]. In this work, the values found for both were 5.74 m and 567.64 m², respectively.

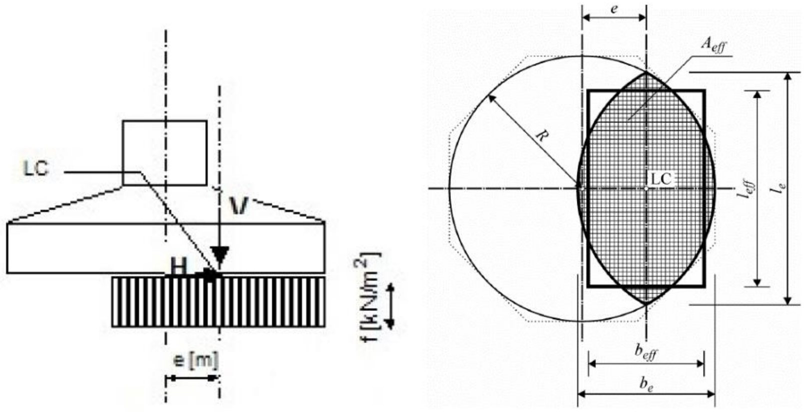

Figure 3. Left: Loading under idealised conditions. Right: Effective foundation area marked out [9].

When a torque M_{Zd} is applied to the foundation, the interaction between it and H_d can be accounted for by replacing H_d and M_{zd} with an equivalent horizontal force $H_{d'}$. The foundation's bearing capacity must, therefore, be assessed for the pair ($H_{d'}$, V_d) instead of (H_d, V_d) [9]. The spreadsheets made for this calculation showed, however, that the difference between $H_{d'}$ and H_d is less than 1%. $H_{d'}$ was used to verify the horizontal sliding resistance. The ratio between $H_{d'}$ and the horizontal sliding resistance H_{res} was equal to 0.42 (following the formulation presented in [9]). Consequently, the structure is resisting horizontal sliding.

Finally, Brinch Hansen's formula for drained soils from DNVGL-ST-0126 [9] was used to calculate the bearing capacity of the soil. Multiplying the soil reaction stress, equal to 375.4 kPa, by the effective area of the foundation, the total bearing capacity (2.13E+05 kN) is acquired. A comparison was made between this value and V_d. As the value found was 0.535 (< 1), it is concluded that the structure is safe in terms of soil capacity.

4 Fatigue Limit State

Fatigue analysis is a fundamental design criterion in a structural system subjected to a wide variety of cyclical loads, such as a wind turbine. SIMA-RIFLEX [10] generated the stress times series for each of the environmental conditions derived within DLC 1.2 (Table 2) for the foundation's points of interest. Unlike steel welded joints, where the focus is in stress range, concrete is strongly influenced by the mean stress load to which it is subjected. Markov Matrix method is applied to consider the mean stress in fatigue damage evaluation [9]. The Markov Matrix consists of another way to compute the results obtained from the Rainflow Counting method. Instead of calculating the stress range ($\Delta\sigma$) and the number of cycles until failure (N), this matrix provides the local maximums (σ_{max}, σ_{min}) of each cycle and the N number of cycles (Fig. 4). Thus, it is possible to consider the mean stress load indirectly [17]. In parallel, Palmgren-Miner rule assesses the fatigue damage using an S-N curve for concrete, as recommended by DNGL-ST-C502 [15].

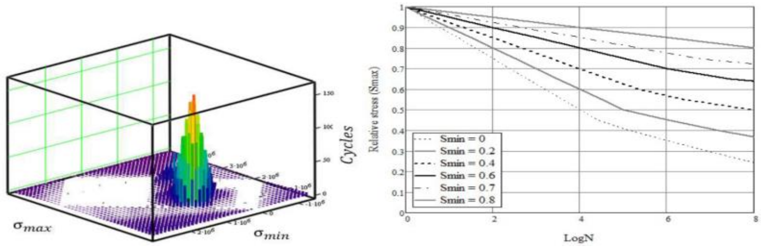

Figure 4. Left: Markov Matrix. Right: S-N curve [17].

WAFO toolbox [18] performed the post-processing of the dynamic analyses. It made use of the Rainflow algorithm, which allowed the extraction of local maximums to serve as input in the implemented S-N curve available in the DNVGL standard [15]. These curves were also used in the work of Gomes [17] and Nadal [19] and have a failure function given by eq. (1):

$$\log_{10} N = C_1\left(1-\frac{\sigma_{max}}{C_5\frac{f_{cn}}{\gamma_m}}\right)\Big/\left(1-\frac{\sigma_{min}}{C_5\frac{f_{cn}}{\gamma_m}}\right), \tag{1}$$

where γ_m is the concrete's material factor, taken as 1.5; the factor C_1 is equal to 8.0 (most conservative value [15]); factor C_5 is equal to 0.8 [15]; σ_{max} and σ_{min} correspond to the local maximum and minimum stress, and f_{cn} is the in situ compressive strength of concrete given by eq. (2):

$$f_{cn} = f_{ck}\left(1-\frac{f_{ck}}{600}\right), \tag{2}$$

where f_{ck}, in MPa, corresponds to the characteristic compressive strength of concrete. When $\log_{10}N$ is greater than X, eq. (3), the fatigue life can be increased by a factor C_2, given by eq. (4).

$$X = C_1\Big/\left[\left(1-\frac{\sigma_{min}}{C_5\frac{f_{cn}}{\gamma_m}}\right)+0.1C_1\right], \tag{3}$$

$$C_2 = 1 + 0.2(\log_{10} N - X). \tag{4}$$

As recommended by DNVGL-ST-C502 [15] and according to Gomes [17], all bending moments that would introduce tensile stress in the concrete were set to $\sigma_{min} = 0$. By doing that, it is possible to analyze the concrete on the compression-compression zone.

Figure 5 presents the lifespan of the GBF. For the same reasons described in item 3.1, the critical point chosen for the fatigue analysis is the shaft-base interface. For $f_{ck} = 55$ MPa, the structure's lifespan without safety factors was 4706 years. Therefore, a sensitivity analysis varying the f_{ck} was performed to analyze the lifespan results obtained considering the same stress time series. Changing the value of f_{ck} in eq. (2), and calculating the damage again, it is possible to notice significant changes in the structure's lifespan, reaching eight years for f_{ck} = 35 MPa. The results of the lowest point of the base's central section are shown in Fig. 5 to confirm that the shaft-base interface is the critical point.

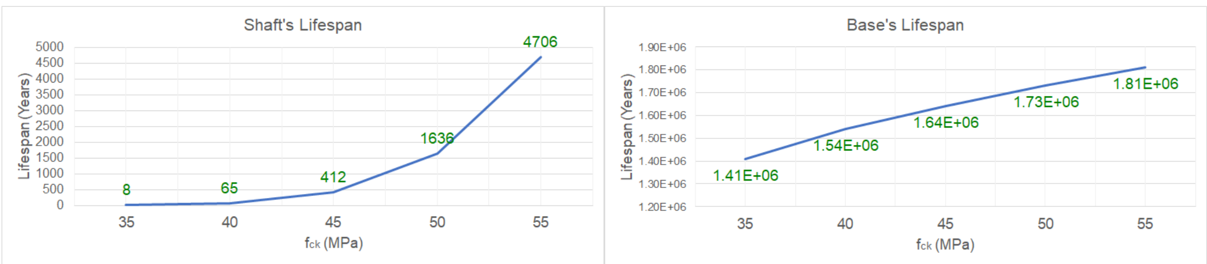

Figure 5. Left: Lifespan results for the shaft. Right: Lifespan results for the base.

5 Conclusions

This work designed a GBF under the action of environmental loads from the Brazilian Northeast coast. A wind turbine is expected to remain in operation between 20 and 30 years. Thus, for the original f_{ck} (= 55 MPa), the model met all the criteria presented in this paper. Considering a safety factor of 3 [9] and a design lifetime of 20 years, all f_{ck} presented in Fig. 5 would be valid except for f_{ck} = 35 MPa. Figure 5 shows how the shaft's lifespan varies exponentially with f_{ck}. Despite not being presented in this work, the abrupt variation in f_{ck} should also cause considerable changes in item 2.1, especially in the adopted reinforcement and in the number of iterations to limit the maximum crack width of the critical section.

Internal tests with SIMA-RIFLEX [10] and the spreadsheets developed in the scope of this work showed that slight changes in the f_{ck} do not contribute significantly to the structure's natural frequencies. Geometric parameters, in particular the base's outer diameter, are decisive in this regard. As mentioned in item 2.3, the spring formulations that define the soil-foundation interaction greatly influence the first modes of vibration, which must be located in the soft-stiff range. Therefore, a suggestion for future work would be more accurate modeling of the soil through finite elements.

For future work, it is intended to evaluate how this foundation interacts with soft soils and what measures can be taken to make them feasible in this situation. Overburden depth, the substitution of local soil, or the adoption of skirts at the base of the foundation [7] are examples of measures that would aim to increase geotechnical capacity, if necessary. Also, geometric discontinuity at the shaft-base interface is a topic to be addressed, as there is a possibility that it is necessary to adopt stress concentration factors for the model presented in this work.

Acknowledgements. The study described in this paper is the result of a partnership between Petrobras and UFRJ and was carried out with resources from the R&D program of the Electricity Sector regulated by ANEEL, under the PD-00553-0045/2016 project titled "Planta Piloto de Geração Eólica Offshore". The authors would also like to express their gratitude to "Coordenação de Aperfeiçoamento de Pessoal de Nível Superior" (CAPES) and "Conselho Nacional de Desenvolvimento Científico e Tecnológico" (CNPq) for the resources destined to the production of this research.

Authorship statement. The authors hereby confirm that they are the sole liable persons responsible for the authorship of this work, and that all material that has been herein included as part of the present paper is either the property (and authorship) of the authors, or has the permission of the owners to be included here.

References

[1] Ministry of Mines and Energy. "Brazilian Energy Review 2020 – Base Year 2019". 2020.
[2] O. A. C. Amarante, D. J. Schultz, R. M. Bittencourt and N. A. Rocha. "Wind/ Hydro Complementary Seasonal Regimes in Brazil". *DEWI Magazine*, vol. 19, pp. 79–86, 2001.
[3] A. R. Silva, F. M. Pimenta, A. T. Assireu and M. H. C. Spyrides. "Complementary of Brazil's hydro and offshore wind power". *Renewable and Sustainable Energy Reviews*, vol. 56, *Elsevier Applied Science*, pp. 413–427, 2015.
[4] Wind Europe. "Offshore Wind in Europe – Key trends and statistics 2019". 2020.
[5] G. Spagnoli and L. Weixler. "Support for Offshore Monopile Installation through the Trench Cutter Technology". Trans RINA, vol. 155, Part A3, *The International Journal of Maritime Engineering*, 2013.
[6] H.C. Barthelemy, *et al*. "Grouted Driven Piles: An Economic and Safe Alternate for Pile Foundations". *19th Annual Offshore Technology Conference*, USA, 1987.
[7] R. Koekkoek. "Gravity Base Foundations for Offshore Wind Turbines". Master thesis, Delft University of Technology, Netherlands, 2015.
[8] C. Bak, *et al*. "DTU Wind Energy Report-I-0092: Description of the DTU 10 MW Reference Wind Turbine". Denmark, 2013.
[9] DNVGL. "DNVGL-ST-0126: Support structures for wind turbines". Norway, 2016.
[10] Sintef Ocean. "RIFLEX 4.10.3 Theory Manual". 2017.
[11] Brazilian Association of Technical Standards. "NBR-6118: Projeto de estruturas de concreto – Procedimento". Brazil, 2014.
[12] DNVGL. "DNVGL-ST-0437: Loads and site conditions for wind turbines". Norway, 2016.
[13] G. Nogueira. "Evaluation of the Behavior of Fixed Offshore Wind Turbines of the Monopile Type". Master thesis, Federal Univeristy of Rio de Janeiro, Brazil, 2019.
[14] B. J. Jonkman and L. Kilcher. "Turbsim user's guide: version 1.06.00. Draft version". National Renewable Energy Laboratory – NREL, USA, 2012.
[15] DNVGL. "DNVGL-ST-C502: Offshore concrete structures". Norway, 2018.
[16] S. D. Cardoso. "Pcalc! v1.4: Análise de Pilares de Concreto Armado – Flexão Composta Oblíqua". 2014.
[17] F. A. Gomes. "Fatigue Analysis of na Offshore Wind Turbine of the Monopile Type with Grouted Connection". Master Thesis, Federal University of Rio de Janeiro, Brazil, 2019.
[18] P. A. Brodtkorb, *et al*. "WAFO – A Matlab toolbox for analysis of random waves and loads". *10th International Offshore and Polar Engineering Conference*, International Society of Offshore and Polar Engineers, 2000.
[19] A. O. Nadal. "Time Domain Simulation Parameters for Fatigue Assessment of an Offshore Gravity Based Wind Turbine". Master Thesis, Norwegian University of Science and Technology, Norway, 2018.